

# Critical-time metric for risk analysis against sharp input anomalies: computation and application case study

Arthur Perodou<sup>a,\*</sup>, Christophe Combastel<sup>b</sup>, Ali Zolghadri<sup>b</sup>

<sup>a</sup>*Ampere-lab, Univ. Lyon, Ecole Centrale de Lyon, INSA Lyon, Univ. Claude Bernard Lyon 1, CNRS UMR 5005, Ecully, 69130, France*

<sup>b</sup>*IMS-lab, Univ. Bordeaux, CNRS UMR 5218, Talence, 33400, France*

---

## Abstract

This paper investigates the critical-time criteria as a security metric for controlled systems subject to sharp input anomalies (attack, fault), characterized by having high impact in a reduced amount of time (e.g. denial-of-service, attack by upper saturation). The critical-time is the maximal time-horizon for which a system can be considered to be safe after the occurrence of an anomaly. This metric is expected to be useful for risk analysis and treatment (prevention, detection, mitigation). In this work, the computational problem of the critical-time for uncertain linear systems and several classes of sharp input anomalies, depending on the input channel and the set of abnormal signal values, is formulated based on the quadratic constraints (QC) framework, representing sets by the intersection of QC inequalities and equalities. An iterative LMI-based algorithm is then proposed to provide an under-estimate of the critical-time. Finally, the potential of the critical-time as a metric for defense design is illustrated and discussed on the quadruple-tank case study through different relevant scenarios.

### *Keywords:*

Secure Control, Cyber-Physical Systems, Critical-time, Sharp Anomalies, Quadratic Constraints

---

\*Corresponding author. Contact: arthur.perodou@ec-lyon.fr

## 1. Introduction

The ever-increasing integration of information and communication technologies into engineering systems has led to the emergence of the cyber-physical systems (CPS) vision [1], where cyber and physical parts are jointly co-designed. The Achilles heel of any CPS is widely recognized to be its fragility, i.e. its vulnerability to adverse anomalous events such as physical faults and cyber intrusions that may result in catastrophic cascading consequences and unacceptable scenarios [2]. Although historically a topic of the Computer Science community, these anomalous events have highlighted the need to consider the interconnection between the cyber and physical parts, and it is now recognized that defense design cannot be based solely on traditional IT security methods [3]. Therefore, over the past decade, the System and Control community has developed numerous methods to address the problem of security in controlled systems [2, 4, 5].

A key point for CPS security is to develop metrics that can be used efficiently for risk analysis and treatment (prevention, detection, mitigation) [6, 4]. In that sense, several criteria have been developed in order to quantify the physical impact of cyber-physical attacks. For instance, the maximum impact of stealthy attacks on the quadratic objective function of an optimal control problem is computed and used for the design of the controller and the detector in [7, 8, 9]; the distance of the set of reachable states by stealthy attacks to a safe/critical region is evaluated and used as a prevention tool in [6, 10] or as criteria for controller and detector design in [11]; the maximum number of attacks on actuators and sensors under which the state can still be estimated is proposed jointly with an associated mitigation scheme in [12]; a metric defined by the ratio of the energy required by the attack to deviate the system from the state trajectory over the control energy needed for recovery is reported in [13].

Recently, a new security metric named critical-time was proposed in [14]. The critical-time is the maximal time-horizon for which a system is considered to be safe after the occurrence of an anomaly (attack, fault), that is the system is not in a critical state allowing to recover to a nominal mode or to reconfigure for a safe stop. The interest of the critical-time is manifold. First, this time-based metric can be usefully included in each stage of the risk management framework. In the risk analysis stage, it identifies system vulnerabilities and anomalies with the greatest impact, associated with a low critical-time. In the risk treatment stage, this metric may be

used to prevent anomalies, associated then with high or even infinite critical-time [10], to provide a design objective for the synthesis of anomaly detectors [15, 16] or for the development of a mitigation mechanism, such as reconfigurable control [17], dissipation block activation [18] or software rejuvenation [19]. Moreover, maximizing the critical-time will leave extra-time for defense mechanisms, including human operators, to detect and mitigate anomalies. This may be achieved by tuning remaining degrees of freedom, as in a rational security allocation approach [4]. Furthermore, an originality is to consider the more general concept of anomaly, instead of only attacks, as the impact of certain attacks and faults can be modeled in a similar way (see for instance [20]). This especially allows this metric to be integrated in a secure and safe approach where both attacks and faults are considered. In particular, the critical-time generalizes the detection and reconfiguration delays classically used in the fault-management literature [15, 17].

In this paper, the critical-time metric for controlled systems subject to sharp input anomalies, characterized by having high impact in a reduced amount of time (e.g. denial-of-service, attack by upper saturation), is investigated. The associated computational problem for an uncertain linear discrete-time model is addressed by taking advantage from the quadratic constraints (QC) framework, representing sets by the intersection of QC inequalities and equalities. This problem is reformulated in terms of LMI (Linear Matrix Inequality) [21] and an iterative LMI-based algorithm is proposed to provide an under-estimate of the critical-time. Unlike [14], limited to the worst-case scenario where the attacker has full control of the inputs, the class of sharp input anomalies is significantly extended. By explicitly modeling the controller, sharp anomalies that only impact some inputs, and not all of them, can be considered. In addition, the inclusion of quadratic constraint equalities (QCE) allows for considering specific sharp anomalies, such as denial-of-service (DoS) or attack by upper saturation. Moreover, this paper relaxes the assumption on the initial state which is assumed now to be uncertain, leading to a more practical and robust result. Finally, the potential of the critical-time metric for defense design is thoroughly illustrated on the quadruple-tank case study [22] through different scenarios. In particular, it is shown how the critical time can be maximized by properly selecting the remaining degrees of freedom, leaving extra-time for defense mechanisms.

The paper is organized as follows. In Section 2, the QC framework for convex set representations is introduced. In Section 3, the critical-time computation problem of a controlled system, with an uncertain discrete-time

linear model, subject to sharp input anomalies is formulated. Section 4 demonstrates how the computation can be performed based on LMI optimization. Finally, the approach is applied on the quadruple-tank case study in Section 5, while Section 6 provides some concluding remarks.

*Notations.* Lower (upper) case letters are used for vectors (matrices).  $\mathbb{R}^+$  denotes the set of non-negative real numbers and  $\mathbb{R}^{n \times m}$  the set of real-valued matrices of size  $n \times m$ .  $I_n$  and  $0_{n \times m}$  are respectively the identity matrix of  $\mathbb{R}^{n \times n}$  and the zero matrix of  $\mathbb{R}^{n \times m}$ . The subscripts are omitted when obvious from the context.  $X^T$  stands for transpose of  $X$  while  $M >$  (resp.  $\geq$ )  $0$  denotes positive (semi-) definiteness. For the sake of brevity,  $[[k_1, k_2]]$  refers to the integers from  $k_1$  to  $k_2$   $z_{[[k_1, k_2]]} := [z_{k_1}^T \dots z_{k_2}^T]^T$ . Bold characters denote decision variables in a design problem or optimization variables in an optimization problem.

## 2. Convex Set Representation by Quadratic Constraints Intersection

This section introduces and motivates the choice of Quadratic Constraints (QC) as a computational framework. First, QC can be used to represent a large class of convex sets. In addition, this framework allows for considering the intersection of these sets, without explicitly computing it. Finally, its link with LMI optimization provides efficient numerical methods.

### Definition 1.

Consider a quadratic function  $\sigma_S(\cdot)$  defined by:

$$\forall z \in \mathbb{R}^{n_z}, \quad \sigma_S(z) := \begin{bmatrix} z \\ 1 \end{bmatrix}^T S \begin{bmatrix} z \\ 1 \end{bmatrix}$$

where  $S = S^T \in \mathbb{R}^{(n_z+1) \times (n_z+1)}$ . A vector  $z \in \mathbb{R}^{n_z}$  is said to satisfy a QC associated with  $\sigma_S$  if  $\sigma_S(z) \geq 0$  holds. In addition,  $z \in \mathbb{R}^{n_z}$  is said to satisfy a QC equality (QCE) associated with  $\sigma_S$  if  $\sigma_S(z) = 0$  holds.

It can be inferred from Definition 1 that the most common classes of convex sets classically used [23] can be exactly expressed in the QC framework. For example, an ellipsoid and a degenerated ellipsoid, such as an halfspace, is inherently represented as a single QC [24]. The set  $\mathcal{E}$  defined by

$$\mathcal{E} := \{z \in \mathbb{R}^{n_z} \mid \sigma_{P_{\mathcal{E}}}(z) \geq 0\}, \quad P_{\mathcal{E}} := \begin{bmatrix} Q & s \\ s^T & r \end{bmatrix}$$

leads to an ellipsoid when  $Q < 0$ , a degenerated ellipsoid when  $Q \leq 0$  and a halfspace when  $Q = 0$ . The intersection of QCs offers then the possibility to represent the intersection of ellipsoids and degenerated ellipsoids. In particular, a polytope in  $H$ -representation  $\mathcal{H} := \{z \in \mathbb{R}^{n_z} \mid Hz \leq h\}$ ,  $h \in \mathbb{R}^{n_h}$ , is represented by the intersection of halfspaces:

$$\mathcal{H} = \bigcap_{i=1}^{n_h} \left\{ z \in \mathbb{R}^{n_z} \mid \sigma_{P_{\mathcal{H}_i}}(z) \geq 0 \right\}, \quad P_{\mathcal{H}_i} := \begin{bmatrix} 0 & H_i^T \\ H_i & 2h_i \end{bmatrix}$$

where  $H_i$  the  $i$ th line of  $H$  and  $h_i$  the  $i$ th element of  $h$ . Moreover, a QCE especially enables to represent convex sets defined by a linear equality, such as a hyperplane  $\mathcal{HP} := \{z \in \mathbb{R}^{n_z} \mid a^T z = b\}$  where  $a \in \mathbb{R}^{n_z}$  and  $b \in \mathbb{R}$ . Planes, that are the intersection of hyperplanes, can then be represented by the intersection of QCEs. Finally, considering the intersection of both QCs and QCEs significantly extends the scope. For instance, a zonotope  $\mathcal{Z} = \{z \in \mathbb{R}^{n_z} \mid z = c + G\lambda, \lambda \in [-1, 1]^{n_\lambda}\}$  can be expressed as the intersection of  $n_z$  hyperplanes and  $n_\lambda$  degenerated ellipsoids, i.e. QCEs and QCs. Zonotope bundles, that are sets defined as the intersection of zonotopes, are also exactly represented, as well as constrained zonotopes  $\mathcal{CZ} = \{z \in \mathbb{R}^{n_z} \mid z = c + G\lambda, D\lambda + d = 0, \lambda \in [-1, 1]^{n_\lambda}\}$  which result from the intersection of a zonotope with hyperplanes. Up to the numerical reliability of optimization solvers, QCs provide a useful design framework to exactly define and operate over a wide class of convex sets.

An important result of the QC framework is the S-procedure lemma that provides a sufficient condition, in the form of a feasibility optimization problem under LMI constraints, to test the satisfaction of a QC by a set of vectors defined by the intersection of QCs [21, Chap. 2]. The next lemma provides an adapted version when a QC is checked over multiple QCs and QCEs (see [25, Theorem 2.3.3]).

**Lemma 1** (S-procedure for intersection of QCs and QCEs).

*Consider  $(N + 1)$  QCs associated with  $\sigma_S, \sigma_{P_1}, \dots, \sigma_{P_N}$ , and  $M$  QCEs associated with  $\sigma_{Q_1}, \dots, \sigma_{Q_M}$ .*

*Then (ii)  $\Rightarrow$  (i).*

(i) *The QC  $\sigma_S(z) \geq 0$  holds for all  $z \in \mathbb{R}^{n_z}$  such that*

$$\begin{aligned} \forall p \in \llbracket 1, N \rrbracket & \quad \sigma_{P_p}(z) \geq 0 \\ \forall q \in \llbracket 1, M \rrbracket & \quad \sigma_{Q_q}(z) = 0 \end{aligned}$$

(ii)  $\exists \{\boldsymbol{\tau}_p \in \mathbb{R}^+\}_{p=1}^N, \exists \{\boldsymbol{\mu}_q \in \mathbb{R}\}_{q=1}^M$ , such that

$$S - \sum_{p=1}^N \boldsymbol{\tau}_p P_p - \sum_{q=1}^M \boldsymbol{\mu}_q Q_q \geq 0 \quad (1)$$

*Remark 1.* The scalars  $\boldsymbol{\tau}_p$  and  $\boldsymbol{\mu}_q$ , classically called multipliers, are the optimization variables in the constraint (1), leading then to a feasibility problem over LMI constraints.

### 3. Problem Setting

#### 3.1. Nominal system description

Consider an uncertain linear discrete-time system ( $\Sigma$ ):

$$(\Sigma) \begin{cases} x_{k+1} = A_\Sigma x_k + B_\Sigma u_k^a + W_\Sigma w_k, & u_k^a \in \mathcal{U} \\ y_k = C_\Sigma x_k + V_\Sigma v_k \end{cases}$$

where  $x_k \in \mathbb{R}^n$  is the system state evaluated at time step  $k$ ,  $u_k^a \in \mathbb{R}^m$  the applied input and  $y_k$  the measured output. The applied input  $u_k^a$  is constrained to belong to the input-limitation set  $\mathcal{U} \subseteq \mathbb{R}^m$ . The vectors  $w_k \in \mathbb{R}^{n_w}$  and  $v_k \in \mathbb{R}^{n_v}$  represent additive state disturbances and measurement noises.

The system ( $\Sigma$ ) is interconnected, through a communication network, to a controller ( $\mathcal{K}$ ) modeled as:

$$(\mathcal{K}) \begin{cases} \xi_{k+1} = A_K \xi_k + B_K y_k \\ u_k = C_K \xi_k + D_K y_k \end{cases}$$

where  $\xi_k \in \mathbb{R}^l$  is the controller state and  $u_k \in \mathbb{R}^m$  is the controller output. Under normal conditions,  $u_k^a = u_k$ .

#### 3.2. Sharp input anomalies

In this paper, sharp anomalies, producing severe impact in a reduced amount of time, on inputs are considered. This especially includes anomalies such as sudden actuator failures, DoS and attack by saturation. From a security point of view, sharp attacks result typically from adversaries with little knowledge of the overall system, and may be accomplished from different manners (fragility of a communication network protocol, communication

channel jamming, direct attack on the controller, or even resulting from false-data measurements) [26]. Unlike the more sophisticated class of stealthy attacks, sharp anomalies may be detected by a passive detection scheme, for instance based on an observer or using a  $\chi^2$ -detector [2, 4].

The anomalies impact on the applied input is modeled as

$$u_k^a = \Gamma_u u_k + \Gamma_a a_k$$

where  $a_k \in \mathcal{A}$  is an unknown signal and  $\mathcal{A} \subseteq \mathbb{R}^{m_a}$  the set of possible values for  $a_k$ , while  $\Gamma_u \in \mathbb{R}^{m \times m}$  and  $\Gamma_a \in \mathbb{R}^{m \times m_a}$  denote the input channels on which the anomalies appear, and are typically binary-valued  $\{0, 1\}$ -matrices. A large class of sharp input anomalies can be modeled by the triplet  $(\Gamma_u, \Gamma_a, \mathcal{A})$ . For instances,  $(\Gamma_u, \Gamma_a, \mathcal{A}) = (0, I, \mathcal{U})$  models the worst-case scenario where an adversary may apply any admissible input,  $(\Gamma_u, \Gamma_a, \mathcal{A}) = (0, I, 0)$  may be associated with a DoS,  $(\Gamma_u, \Gamma_a) = (I, I)$  models additive input faults or data-injection attacks, that are with saturation objective when  $\mathcal{A} = \{a = \alpha \cdot u_{max}^a\}$  where  $u_{max}^a$  the maximum admissible input and  $\alpha \in \mathbb{R}$  a large number, while

$$\Gamma_u = \begin{bmatrix} I & 0 & 0 \\ 0 & 0_{1 \times 1} & 0 \\ 0 & 0 & I \end{bmatrix} \quad \text{and} \quad \Gamma_a = \begin{bmatrix} 0 & 0 & 0 \\ 0 & 1 & 0 \\ 0 & 0 & 0 \end{bmatrix}$$

model anomalies that appear on the  $i^{th}$  input channel. Normal operating conditions are obtained when  $(\Gamma_u, \Gamma_a) = (I, 0)$ .

### 3.3. Controlled system subject to sharp input anomalies

The dynamics of the interconnected system  $(\Sigma - \mathcal{K})$  subject to input anomalies (Fig. 1) is then given by:

$$(\Sigma - \mathcal{K}) \begin{cases} \bar{x}_{k+1} = A\bar{x}_k + W\bar{w}_k + B_a a_k \\ u_k^a = C_u \bar{x}_k + V_u \bar{w}_k + \Gamma_a a_k, \quad u_k^a \in \mathcal{U} \end{cases} \quad (2)$$

where  $\bar{x}_k := [x_k^T \quad \xi_k^T]^T$ ,  $\bar{w}_k := [w_k^T \quad v_k^T]^T$  and

$$A = \begin{bmatrix} A_\Sigma + B_\Sigma \Gamma_u D_K C_\Sigma & B_\Sigma \Gamma_u C_K \\ B_K C_\Sigma & A_K \end{bmatrix}, \quad B_a = \begin{bmatrix} B_\Sigma \Gamma_a \\ 0 \end{bmatrix}$$

$$W = \begin{bmatrix} W_\Sigma & B_\Sigma \Gamma_u D_K V_\Sigma \\ 0 & B_K V_\Sigma \end{bmatrix}, \quad C_u = \Gamma_u [D_K C_\Sigma \quad C_K]$$

$$V_u = \Gamma_u [0 \quad D_K V_\Sigma]$$

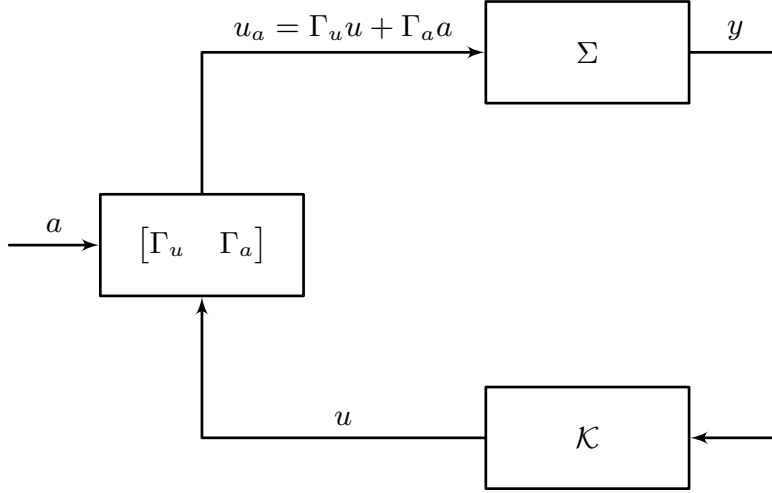


Figure 1: Controlled system subject to sharp input anomalies

This interconnected system  $(\Sigma - \mathcal{K})$  is provided with a safety set  $\bar{\mathcal{S}} \subseteq \mathbb{R}^{n+l}$ , i.e. a set of states  $\bar{x}_k$  for which  $(\Sigma - \mathcal{K})$  is considered to be safe at each time step  $k$ . For the ease of computation, and without loss of generality, it is assumed that the anomalies start from  $k_a = 0$ . The initial state  $\bar{x}_0$  is assumed to belong to a known and safe set  $\bar{\mathcal{X}}_0 \subseteq \bar{\mathcal{S}}$ , and the additive uncertainties  $\bar{w}_k$  to a bounded set  $\bar{\mathcal{W}} \subseteq \mathbb{R}^{n_w+n_v}$ .

The defense objective is to design off-line a strategy such that safe operation is preserved after the occurrence of an anomaly. In this perspective, an (under)-estimation of the critical-time, that is the maximum time window allowed before the system leaves the safety set, appears as a crucial information to be provided to the defense designer.

#### 3.4. Problem formulation

The problem considered in this paper is the computation of the critical-time for the interconnected system (2) subject to sharp input anomalies defined by  $(\Gamma_u, \Gamma_a, \mathcal{A})$ , based on the QC framework. To this end, the safety set  $\bar{\mathcal{S}}$  is assumed to be exactly represented or inner-approximated by the intersection of QCs (Definition 1):

$$\bigcap_{s=1}^{n_{\bar{\mathcal{S}}}} \bar{\mathcal{S}}_s \subseteq \bar{\mathcal{S}}, \quad \bar{\mathcal{S}}_s := \{\bar{x} \in \mathbb{R}^{n+l} \mid \sigma_{\bar{\mathcal{S}}_s}(\bar{x}) \geq 0\} \quad (3)$$



and the initial set  $\bar{\mathcal{X}}_0$ , the input-limitation set  $\mathcal{U}$ , the deviation set  $\bar{\mathcal{W}}$  and the anomaly-impact set  $\mathcal{A}$  are exactly represented or over-approximated by the intersection of QCs and QCEs:

$$\bar{\mathcal{X}}_0 \subseteq \left\{ \bigcap_{g=1}^{n_{\bar{\mathcal{X}}_0}} \bar{\mathcal{X}}_g \right\} \cap \left\{ \bigcap_{h=1}^{m_{\bar{\mathcal{X}}_0}} \bar{\mathcal{X}}_h^e \right\} \quad (4)$$

$$\mathcal{U} \subseteq \left\{ \bigcap_{i=1}^{n_{\mathcal{U}}} \mathcal{U}_i \right\} \cap \left\{ \bigcap_{j=1}^{m_{\mathcal{U}}} \mathcal{U}_j^e \right\} \quad (5)$$

$$\bar{\mathcal{W}} \subseteq \left\{ \bigcap_{p=1}^{n_{\bar{\mathcal{W}}}} \bar{\mathcal{W}}_p \right\} \cap \left\{ \bigcap_{q=1}^{m_{\bar{\mathcal{W}}}} \bar{\mathcal{W}}_q^e \right\} \quad (6)$$

$$\mathcal{A} \subseteq \left\{ \bigcap_{r=1}^{n_{\mathcal{A}}} \mathcal{A}_r \right\} \cap \left\{ \bigcap_{t=1}^{m_{\mathcal{A}}} \mathcal{A}_t^e \right\} \quad (7)$$

with  $\bar{\mathcal{X}}_g := \{\bar{x}_0 \in \mathbb{R}^{n+l} \mid \sigma_{\bar{\mathcal{X}}_g}(\bar{x}_0) \geq 0\}$ ,  $\bar{\mathcal{X}}_h^e := \{\bar{x}_0 \in \mathbb{R}^{n+l} \mid \sigma_{\bar{\mathcal{X}}_h^e}(\bar{x}_0) = 0\}$ ,  $\mathcal{U}_i := \{u^a \in \mathbb{R}^m \mid \sigma_{\mathcal{U}_i}(u^a) \geq 0\}$ ,  $\mathcal{U}_j^e := \{u^a \in \mathbb{R}^m \mid \sigma_{\mathcal{U}_j^e}(u^a) = 0\}$ ,  $\bar{\mathcal{W}}_p := \{\bar{w} \in \mathbb{R}^{n_v+n_w} \mid \sigma_{\bar{\mathcal{W}}_p}(\bar{w}) \geq 0\}$ ,  $\bar{\mathcal{W}}_q^e := \{\bar{w} \in \mathbb{R}^{n_v+n_w} \mid \sigma_{\bar{\mathcal{W}}_q^e}(\bar{w}) = 0\}$ ,  $\mathcal{A}_r := \{a \in \mathbb{R}^{m_a} \mid \sigma_{\mathcal{A}_r}(a) \geq 0\}$ , and  $\mathcal{A}_t^e := \{a \in \mathbb{R}^{m_a} \mid \sigma_{\mathcal{A}_t^e}(a) = 0\}$ .

*Remark 2.* The introduction of QCEs makes possible to exactly represent anomalies impact leading to constant  $a_k$ , such as in the cases of DoS or attack by upper saturation.

The problem can now be stated as follows.

**Problem 1.**

GIVEN the system (2) subject to input anomalies modeled by  $(\Gamma_u, \Gamma_a, \mathcal{A})$ , GIVEN a safety set  $\bar{\mathcal{S}}$ , an initial set  $\bar{\mathcal{X}}_0 \subseteq \bar{\mathcal{S}}$ , an input-limitation set  $\mathcal{U}$  and a deviation set  $\bar{\mathcal{W}}$ , GIVEN the approximation (3)-(7) in the QC framework, FIND the maximal time-index  $\mathbf{k}_f$  such that system (2) is safe over the time-window  $\llbracket 0, \mathbf{k}_f \rrbracket$  for all initial states of  $\bar{\mathcal{X}}_0$ , for all anomalies of  $\mathcal{A}$  resulting in admissible inputs of  $\mathcal{U}$ , and for all elements of  $\bar{\mathcal{W}}$ :

$$\max_{\mathbf{k}_f \in \mathbb{N}} \mathbf{k}_f$$

subject to  $\forall \bar{x}_0 \in \bar{\mathcal{X}}_0, \forall k \in \llbracket 0, \mathbf{k}_f \rrbracket, \forall a_k \in \mathcal{A}$  such that  $u_k^a \in \mathcal{U}, \forall \bar{w}_k \in \bar{\mathcal{W}}, \bar{x}_k \in \bar{\mathcal{S}}$ .

#### 4. Critical-time computation

In this section, first the following problem is solved (Theorem 1): how to check if the state  $\bar{x}_{k_f}$  belongs to the safety set  $\bar{\mathcal{S}}$ , over all initial states of  $\bar{\mathcal{X}}_0$ , occurred anomalies in  $\mathcal{A}$  resulting in admissible inputs in  $\mathcal{U}$ , and uncertainties in  $\bar{\mathcal{W}}$ , for a fixed time-index  $k_f$ . Then, an iterative algorithm (Algorithm 1) is proposed to find the maximal  $k_f$ , providing an underestimate of the critical-time.

##### Theorem 1.

Let  $(\Sigma - \mathcal{K})$  be the interconnected system modeled by (2). Assume that the safety set  $\bar{\mathcal{S}}$ , the initial-state set  $\bar{\mathcal{X}}_0$ , the input-limitation set  $\mathcal{U}$ , the deviation set  $\bar{\mathcal{W}}$  and the anomaly set  $\mathcal{A}$  are provided with QC-based approximations given by (3)-(7). Assume that the time-index  $k_f \in \mathbb{N}$  is fixed.

Then (i)  $\Rightarrow$  (ii).

$$(i) \forall s \in \llbracket 1, n_{\bar{\mathcal{S}}} \rrbracket, \exists \{\phi_{s,g} \in \mathbb{R}^+\}_{g=1}^{n_{\bar{\mathcal{X}}_0}}, \exists \{\varphi_{s,h} \in \mathbb{R}\}_{h=1}^{m_{\bar{\mathcal{X}}_0}}, \forall k \in \llbracket 0, k_f - 1 \rrbracket, \\ \exists \{\pi_{s,k,i} \in \mathbb{R}^+\}_{i=1}^{n_{\mathcal{U}}}, \exists \{\varpi_{s,k,j} \in \mathbb{R}\}_{j=1}^{m_{\mathcal{U}}}, \exists \{\rho_{s,k,p} \in \mathbb{R}^+\}_{p=1}^{n_{\bar{\mathcal{W}}}}, \exists \{\varrho_{s,k,q} \in \mathbb{R}\}_{q=1}^{m_{\bar{\mathcal{W}}}}, \\ \exists \{\sigma_{s,k,r} \in \mathbb{R}^+\}_{r=1}^{n_{\mathcal{A}}}, \exists \{\varsigma_{s,k,t} \in \mathbb{R}\}_{t=1}^{m_{\mathcal{A}}}, \text{ such that:}$$

$$\begin{aligned} & M_{\bar{x}_{k_f}}^T \bar{\mathcal{S}}_s M_{\bar{x}_{k_f}} - M_{\bar{x}_0}^T \left( \sum_{g=1}^{n_{\bar{\mathcal{X}}_0}} \phi_{s,g} \bar{X}_g + \sum_{h=1}^{m_{\bar{\mathcal{X}}_0}} \varphi_{s,h} \bar{X}_h^e \right) M_{\bar{x}_0} \\ & - \sum_{k=0}^{k_f-1} N_{u_k^a}^T \left( \sum_{i=1}^{n_{\mathcal{U}}} \pi_{s,k,i} U_i + \sum_{j=1}^{m_{\mathcal{U}}} \varpi_{s,k,j} U_j^e \right) N_{u_k^a} \\ & - \sum_{k=0}^{k_f-1} E_k^T \left( \sum_{p=1}^{n_{\bar{\mathcal{W}}}} \rho_{s,k,p} \bar{W}_p + \sum_{q=1}^{m_{\bar{\mathcal{W}}}} \varrho_{s,k,q} \bar{W}_q^e \right) E_k \\ & - \sum_{k=0}^{k_f-1} F_k^T \left( \sum_{r=1}^{n_{\mathcal{A}}} \sigma_{s,k,r} A_r + \sum_{t=1}^{m_{\mathcal{A}}} \varsigma_{s,k,t} A_t^e \right) F_k \geq 0 \end{aligned} \quad (8)$$

with

$$\begin{aligned} M_{\bar{x}_k} &= \begin{bmatrix} A^k & P_k & Q_k & 0 \\ 0 & 0 & 0 & 1 \end{bmatrix} \\ P_k &= \begin{bmatrix} A^{k-1}W & \dots & AW & W & 0_{(n+l) \times (k_f-k)(n_v+n_w)} \end{bmatrix} \\ Q_k &= \begin{bmatrix} A^{k-1}B_a & \dots & AB_a & B_a & 0_{(n+l) \times (k_f-k)m_a} \end{bmatrix} \\ N_{u_k^a} &= C_u M_{\bar{x}_k} + V_u E_k + \Gamma_a F_k \end{aligned}$$

where  $P_0 = 0$  and  $Q_0 = 0$ , and  $E_k, F_k$  are such that:

$$E_k z_{k_f} = \begin{bmatrix} \bar{w}_k \\ 1 \end{bmatrix} \quad F_k z_{k_f} = \begin{bmatrix} a_k \\ 1 \end{bmatrix}$$

where  $z_{k_f}^T := \begin{bmatrix} \bar{x}_0^T & \bar{w}_{[0, k_f-1]}^T & a_{[0, k_f-1]}^T & 1 \end{bmatrix}^T$ .

- (ii) The system is safe at time-index  $k_f$ :  $\bar{x}_{k_f} \in \mathcal{S}$  for all initial states  $\bar{x}_0 \in \bar{\mathcal{X}}_0$ , for all anomalies  $a_k \in \mathcal{A}$  resulting in admissible inputs  $u_k^a \in \mathcal{U}$ , and for all deviation elements  $\bar{w}_k \in \bar{\mathcal{W}}$ .

*Proof.* Using the recursive equation (2), it comes

$$M_{\bar{x}_{k_f}} z_{k_f} = \begin{bmatrix} \bar{x}_{k_f} \\ 1 \end{bmatrix} \quad M_{\bar{x}_0} z_{k_f} = \begin{bmatrix} \bar{x}_0 \\ 1 \end{bmatrix} \quad N_{u_k^a} z_{k_f} = \begin{bmatrix} u_k^a \\ 1 \end{bmatrix}$$

Then, by applying Lemma 1 to (8),  $\sigma_{\bar{S}_s}(\bar{x}_f) \geq 0$  holds for all  $\bar{x}_0$ ,  $\{\bar{w}_k\}_{k=0}^{k_f-1}$ , and  $\{u_k^a\}_{k=0}^{k_f-1}$  such that:

$$\begin{aligned} \forall g \in \llbracket 1, n_{\bar{\mathcal{X}}_0} \rrbracket, \sigma_{\bar{\mathcal{X}}_g}(\bar{x}_0) \geq 0 \quad \forall h \in \llbracket 1, m_{\bar{\mathcal{X}}_0} \rrbracket, \sigma_{\bar{\mathcal{X}}_h^e}(\bar{x}_0) = 0 \\ \forall i \in \llbracket 1, n_{\mathcal{U}} \rrbracket, \sigma_{U_i}(u_k^a) \geq 0 \quad \forall j \in \llbracket 1, m_{\mathcal{U}} \rrbracket, \sigma_{U_j^e}(u_k^a) = 0 \\ \forall p \in \llbracket 1, n_{\bar{\mathcal{W}}} \rrbracket, \sigma_{\bar{\mathcal{W}}_p}(\bar{w}_k) \geq 0 \quad \forall q \in \llbracket 1, m_{\bar{\mathcal{W}}} \rrbracket, \sigma_{\bar{\mathcal{W}}_q^e}(\bar{w}_k) = 0 \\ \forall r \in \llbracket 1, n_{\mathcal{A}} \rrbracket, \sigma_{A_r}(a_k) \geq 0 \quad \forall t \in \llbracket 1, m_{\mathcal{A}} \rrbracket, \sigma_{A_t^e}(a_k) = 0 \end{aligned}$$

Thus, for all  $\bar{x}_0 \in \left\{ \bigcap_{g=1}^{n_{\bar{\mathcal{X}}_0}} \bar{\mathcal{X}}_g \right\} \cap \left\{ \bigcap_{h=1}^{m_{\bar{\mathcal{X}}_0}} \bar{\mathcal{X}}_h^e \right\}$ , for all  $\{a_k\}_{k=0}^{k_f-1}$  such that  $a_k \in \left\{ \bigcap_{r=1}^{n_{\mathcal{A}}} \mathcal{A}_r \right\} \cap \left\{ \bigcap_{t=1}^{m_{\mathcal{A}}} \mathcal{A}_t^e \right\}$  and  $u_k^a \in \left\{ \bigcap_{i=1}^{n_{\mathcal{U}}} \mathcal{U}_i \right\} \cap \left\{ \bigcap_{j=1}^{m_{\mathcal{U}}} \mathcal{U}_j^e \right\}$ , and for all  $\{\bar{w}_k\}_{k=0}^{k_f-1}$  such that  $\bar{w}_k \in \left\{ \bigcap_{p=1}^{n_{\bar{\mathcal{W}}}} \bar{\mathcal{W}}_p \right\} \cap \left\{ \bigcap_{q=1}^{m_{\bar{\mathcal{W}}}} \bar{\mathcal{W}}_q^e \right\}$ , one has  $\bar{x}_{k_f} \in \bigcap_{s=1}^{n_{\bar{\mathcal{S}}}} \bar{\mathcal{S}}_s$ . The inclusions (3)-(7) lead to the conclusion.  $\square$

*Remark 3.* Condition (i) is a feasibility optimization problem with LMI constraints. It is then solvable in polynomial-time. This computational advantage comes at the price of the conservatism of condition (i), that is only sufficient. This results from the application of the S-procedure (see [24], and the references therein, for a detailed discussion).

In order to compute the critical-time  $k_c$ , the following iterative LMI-based algorithm (Algorithm 1) is proposed: based on the sufficient condition provided by Theorem 1, the time index  $k_f$  is incremented until no solution is found to the LMI feasibility problem. An under-estimate  $k_f^*$  of the critical-time  $k_c$  is so obtained  $k_f^* \leq k_c$  and ensures that the system is safe at least until the obtained result  $k_f^*$ .

---

**Algorithm 1:** Critical-time computation
 

---

```

1  $k_f \leftarrow 0$ 
2  $t \leftarrow true$ 
3 while  $t$  do
4    $k_f \leftarrow k_f + 1$ 
5    $t \leftarrow isFeasible( \forall s \in \llbracket 1, n_S \rrbracket, \exists \{ \phi_{s,g} \in \mathbb{R}^+ \}_{g=1}^{n_{\bar{x}_0}},$ 
       $\exists \{ \varphi_{s,h} \in \mathbb{R} \}_{h=1}^{m_{\bar{x}_0}}, \forall k \in \llbracket 0, k_f - 1 \rrbracket, \exists \{ \pi_{s,k,i} \in \mathbb{R}^+ \}_{i=1}^{n_u},$ 
       $\exists \{ \varpi_{s,k,j} \in \mathbb{R} \}_{j=1}^{m_u}, \exists \{ \rho_{s,k,p} \in \mathbb{R}^+ \}_{p=1}^{n_{\bar{w}}}, \exists \{ \varrho_{s,k,q} \in \mathbb{R} \}_{q=1}^{m_{\bar{w}}},$ 
       $\exists \{ \sigma_{s,k,r} \in \mathbb{R}^+ \}_{r=1}^{n_A}, \exists \{ \varsigma_{s,k,t} \in \mathbb{R} \}_{t=1}^{m_A},$  such that (8) holds. )
6   /* true if a solution is found /*
7    $k_f \leftarrow k_f - 1$ 
8   return  $k_f$ 

```

---

## 5. Case study - the quadruple-tank system

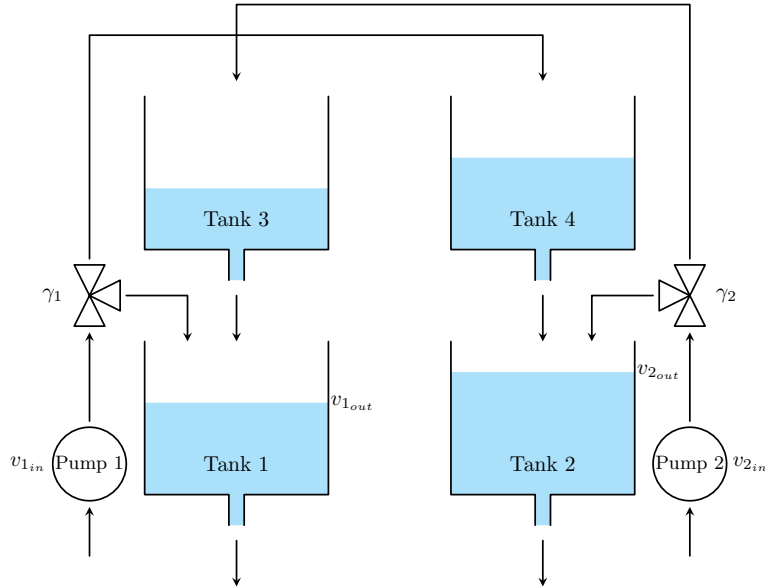


Figure 2: The quadruple-tank system

The quadruple-tank system (Fig. 2) originally described in [22], is considered to illustrate the benefits of the critical-time. This benchmark has

been used in the CPS security literature for simulating cyber-attacks, evaluating their physical impacts and developing counter-measures (see [6, 27] for instance). It consists of four tanks with bottom outlet holes, arranged such that tank 3 is above tank 1 and tank 4 above tank 2. The inputs are the voltages  $v_{1in}, v_{2in}$  applied to two pumps, and the outputs are the voltages  $v_{1out}, v_{2out}$  from level measurement devices of tanks 1 and 2. The input liquid from pump 1 (resp. pump 2) is split into tank 1 and 4 (tank 2 and 3) using a valve with coefficient  $\gamma_1 \in (0, 1)$  (resp.  $\gamma_2 \in (0, 1)$ ). The system is modeled as follows:

$$\begin{cases} \dot{h}(t) = A_P \sqrt{h(t)} + B_P(\gamma_1, \gamma_2)v_{in}(t) \\ v_{out}(t) = C_P h(t) + d(t) \end{cases} \quad (9)$$

where  $h = [h_1 \ h_2 \ h_3 \ h_4]^T$ ,  $h_i$  the liquid level of tank  $i$ ,  $v_{in} = [v_{1in} \ v_{2in}]^T$ ,  $v_{out} = [v_{1out} \ v_{2out}]^T$  and  $d$  the sensor noise. The matrices  $A_P$  and  $C_P$  depend on constant physical parameters of the system, while  $B_P(\gamma_1, \gamma_2)$  is an affine matrix-valued function. See [22] for numerical values.

Due to physical limitations of the pumps, the inputs  $v_{1in}$  and  $v_{2in}$  belong to  $[v_{min}, v_{max}] = [0 \text{ V}, 10 \text{ V}]$ . Moreover, for safety reasons, the levels  $h_1$  and  $h_2$  are constrained to belong to  $[h_{12min}, h_{12max}] = [9 \text{ cm}, 20 \text{ cm}]$  and the levels  $h_3$  and  $h_4$  to  $[h_{34min}, h_{34max}] = [0.1 \text{ cm}, 5 \text{ cm}]$ . In particular, this prevents the tanks to overflow or to be empty, and keeps a minimum output flow for tanks 1 and 2.

The system is remotely controlled through a communication network by PI controllers, that compute the control input  $v_c$  from a reference signal  $r$  and measurement  $v_{out}$  such as  $v_{ic} = K_i(1 + \frac{1}{T_{i,s}})(r_i - v_{iout})$  where  $K_1 = 3$ ,  $K_2 = 2.7$ ,  $T_1 = 30s$ ,  $T_2 = 40s$ . The control objective is to set  $h_1$  and  $h_2$  to  $h_1^0 = 12.4 \text{ cm}$  and  $h_2^0 = 12.7 \text{ cm}$ . Anomalies are assumed to appear when the process is at a stationary operating point  $(h^0, v_{in}^0)$ . It is known [22] that, given  $(h_1^0, h_2^0)$ , the values of  $h_3^0, h_4^0$  and  $v_{in}^0$  are fully determined by the valves coefficients  $(\gamma_1, \gamma_2)$ . The choice of  $(\gamma_1, \gamma_2)$  impacts then both the operating point and the system dynamics. Thus, the aim is to study the influence of  $(\gamma_1, \gamma_2)$  on the critical-time. In addition to evaluate the time allowed to defense mechanism given a couple  $(\gamma_1, \gamma_2)$ , this provides a means to select couples with high critical-time. To this end, the critical-time is computed for a finite number of arbitrarily-chosen  $\gamma_1 \in [0.65, 0.75]$ ,  $\gamma_2 \in [0.55, 0.65]$ .

### 5.1. Uncertain linear discrete-time approximation

For each couple  $(\gamma_1, \gamma_2)$ , the corresponding model (9) is linearized around the associated operating point  $(h^0, v_{in}^0)$ . Then, using the zero-order hold method with a sampling period of 1s, the model (2) is obtained, where  $\bar{w}_k$  represents the deviation between (9) and the approximation, especially resulting from linearization-and-discretization errors and sensor noise. Based on several simulations, the set  $\bar{\mathcal{W}}$  is over-approximated (see Fig. 3) by the intersection of two degenerated ellipsoids  $\bar{\mathcal{W}}_1$  and  $\bar{\mathcal{W}}_2$ ,

$$\bar{\mathcal{W}}_1 = \begin{bmatrix} Q_{\bar{\mathcal{W}}_1} & 0 & s_{\bar{\mathcal{W}}_1} \\ 0 & 0 & 0 \\ s_{\bar{\mathcal{W}}_1}^T & 0 & r_{\bar{\mathcal{W}}_1} \end{bmatrix} \quad \bar{\mathcal{W}}_2 = \begin{bmatrix} Q_{\bar{\mathcal{W}}_2} & 0 & s_{\bar{\mathcal{W}}_2} \\ 0 & 0 & 0 \\ s_{\bar{\mathcal{W}}_2}^T & 0 & r_{\bar{\mathcal{W}}_2} \end{bmatrix}$$

where

$$Q_{\bar{\mathcal{W}}_1} = \begin{bmatrix} -0.567 & 0 & -0.489 & 0 \\ 0 & 0 & 0 & 0 \\ -0.489 & 0 & -0.448 & 0 \\ 0 & 0 & 0 & 0 \end{bmatrix} \quad s_{\bar{\mathcal{W}}_1} = \begin{bmatrix} 0.000263 \\ 0 \\ 0.000433 \\ 0 \end{bmatrix} \quad r_{\bar{\mathcal{W}}_1} = -1.20 \cdot 10^{-8}$$

$$Q_{\bar{\mathcal{W}}_2} = \begin{bmatrix} 0 & 0 & 0 & 0 \\ 0 & -0.611 & 0 & -0.480 \\ 0 & 0 & 0 & 0 \\ 0 & -0.480 & 0 & -0.409 \end{bmatrix} \quad s_{\bar{\mathcal{W}}_2} = \begin{bmatrix} 0 \\ 0.000569 \\ 0 \\ 0.000501 \end{bmatrix} \quad r_{\bar{\mathcal{W}}_2} = -3.70 \cdot 10^{-7}$$

and a hyper-rectangle

$$\{\bar{w} \in \mathbb{R}^6, \bar{w}_{min} \leq \bar{w} \leq \bar{w}_{max}\}$$

with

$$\bar{w}_{min} = - [0.013 \quad 0.0027 \quad 0 \quad 0 \quad 0.137 \quad 0.126]^T$$

$$\bar{w}_{max} = [0.00011 \quad 0.0013 \quad 0.014 \quad 0.0045 \quad 0.143 \quad 0.147]^T$$

Similarly, the initial set  $\bar{\mathcal{X}}_0$  is over-approximated by the hyper-rectangle

$$\{\bar{x}_0 \in \mathbb{R}^6, \bar{x}_{0min} \leq \bar{x}_0 \leq \bar{x}_{0max}\}$$

with

$$\bar{x}_{0min} = - [0.065 \quad 0.047 \quad 0.032 \quad 0.028 \quad 0.066 \quad 0.061]^T$$

$$\bar{x}_{0max} = [0.066 \quad 0.056 \quad 0.044 \quad 0.024 \quad 0.068 \quad 0.077]^T$$

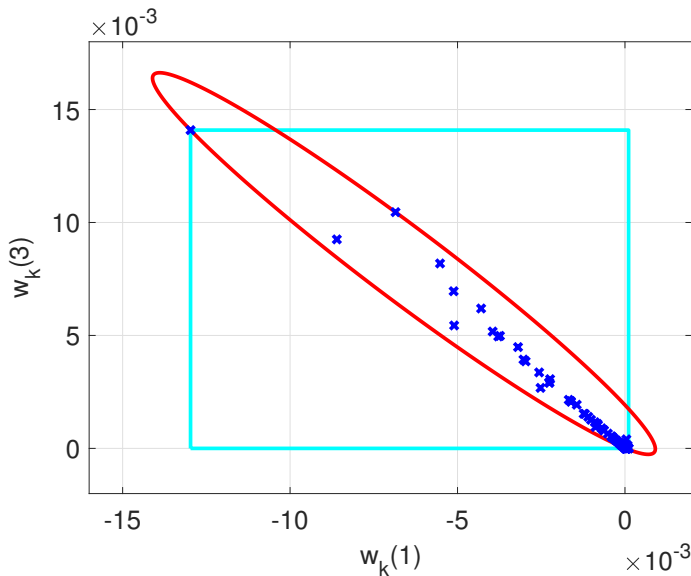


Figure 3: Projection of the hyper-rectangle (cyan solid line) and a degenerated ellipsoid (red solid line) in the plane  $(\bar{w}_k(1), \bar{w}_k(3))$ . Blue crosses denote samples coming from simulations. The intersection of the rectangle and the ellipse includes the whole set of crosses.

## 5.2. Critical-time computation and usage

Algorithm 1 is now applied to estimate the critical-time in three scenarios. The computation is performed using MATLAB R2022b, using the semidefinite mode of the CVX package [28] with the solver MOSEK [29], on a computer with 4-core 3.00 GHz CPU and 32GB RAM.

### 5.2.1. Anomaly-specific scenario

A DoS anomaly, resulting for instance from an unreliable communication network or a jamming cyber-attack, is first considered. When an anomaly is especially risky, an anomaly-specific defense strategy may be designed in the treatment stage. As a case in point, a DoS may be detected using acknowledgment-based communication protocol such as TCP [30]. This anomaly is modeled as  $(\Gamma_u, \Gamma_a, \mathcal{A}) = (0_2, I_2, \mathcal{U}_\gamma)$  where

$$\mathcal{U}_\gamma = \left\{ u \in \mathbb{R}^2, u = \begin{bmatrix} u_{\gamma_1} \\ u_{\gamma_2} \end{bmatrix}, u_{\gamma_i} = 0 - v_{0_i} \right\}$$

recalling that the values of  $v_0$  depends on  $(\gamma_1, \gamma_2)$ . The result is displayed in Table 1. Similarly, an attack-by-upper saturation is considered and the

estimated critical-time is displayed in Table 2. Both results are compared with the result obtained from simulation on the non-linear model (9). It can be especially observed that results from Algorithm 1 and from simulation are close, suggesting a moderate conservatism of the computing approach developed in this paper.

Table 1: Critical-time (s) - DoS (diff. simulation vs algorithm)

$\gamma_1 \backslash \gamma_2$	0.55	0.575	0.60	0.625	0.65
0.65	13	12	10 (+1)	8 (+1)	6 (+1)
0.675	13 (+1)	12 (+1)	11 (+1)	10 (+1)	8 (+1)
0.70	14 (+1)	13	12	11 (+1)	9 (+2)
0.725	10 (+2)	13 (+1)	12 (+1)	12	10 (+1)
0.75	7 (+2)	10 (+1)	11 (+2)	12	11 (+1)

Table 2: Critical-time (s) - Upper Saturation (diff. simulation vs algorithm)

$\gamma_1 \backslash \gamma_2$	0.55	0.575	0.60	0.625	0.65
0.65	9	11	10	8	7
0.675	7	10	13	13 (+1)	13
0.70	6	9	12	12 (+1)	13
0.725	5	8	11	12	12
0.75	4	7	10 (+1)	11	11 (+1)

### 5.2.2. Worst-case scenario

In this scenario, the class of anomalies leading to any admissible input  $(\Gamma_u, \Gamma_a, \mathcal{A}) = (0, I, \mathcal{U})$  is considered. This worst-case scenario may typically happen when an adversary takes full control of the inputs, either through the communication network or by an attack on the controller. In that case, a difficulty is to design a defense strategy for anomalies with opposite impact (see for instance Fig. 4). Indeed, one may observe for instance in Table 1 and Table 2 that the couple  $(\gamma_1, \gamma_2) = (0.70, 0.55)$  leads to the highest critical-time (14 s) for a DoS anomaly but low critical-time (6 s) when considering an



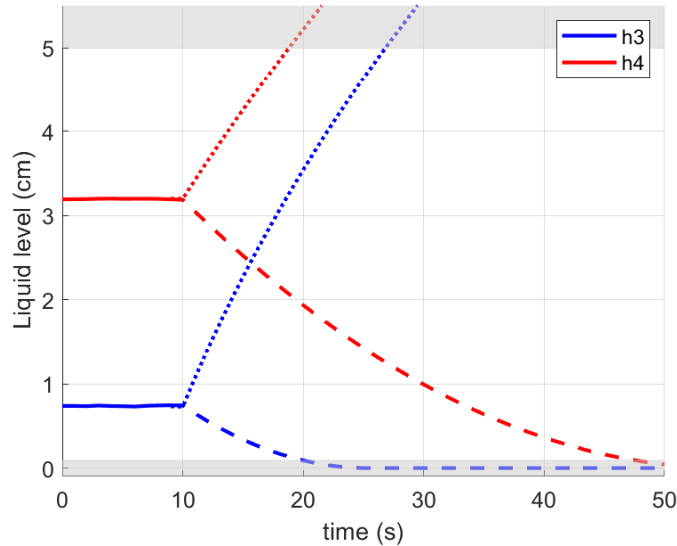


Figure 4: Impact on  $h_3$  and  $h_4$  of a DoS (dashed lines) and an attack by upper saturation (dotted lines) on the quadruple tank system originally at an operating point (solid lines). Grey patches refer to unsafe zones.

attack-by-upper saturation. While an intuitive solution may be found on this example and these two particular anomalies, a suitable trade-off is expected to be more challenging to be made for numerous and diverse anomalies. On the other hand, the computation of the critical-time for all admissible anomalies naturally incorporates this tradeoff, without needing to simulate each element of  $\mathcal{U}$ .

The computed under-estimation of the critical-time in this scenario is displayed in Table 3. In addition, the computational time needed by Algorithm 1 at each iteration is plotted on Fig. 5. As expected, the computational time increases moderately with the time horizon  $k$  and remains tractable. The execution time of Algorithm 1 is 7.3 s on average.

### 5.2.3. Channel-dependent scenario

The classes of anomalies leading to any admissible input for a single input channel is now considered. These are modeled by

$$(\Gamma_{u_1}, \Gamma_{a_1}, \mathcal{A}_1) = \left( \begin{bmatrix} 0 & 0 \\ 0 & 1 \end{bmatrix}, \begin{bmatrix} 1 \\ 0 \end{bmatrix}, \mathcal{U}_1 \right)$$

Table 3: Critical-time (s) - Worst-case scenario

$\gamma_1 \backslash \gamma_2$	0.55	0.575	0.60	0.625	0.65
0.65	9	11	10	8	6
0.675	7	10	11	10	8
0.70	6	9	12	11	9
0.725	5	8	11	12	10
0.75	4	7	10	11	11

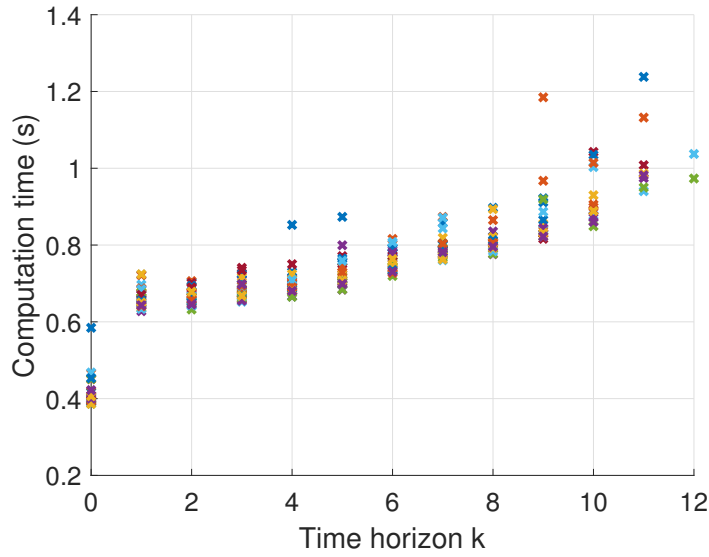


Figure 5: Computational time per iteration in the worst-case scenario

for the first channel  $C_1$  and by

$$(\Gamma_{u_2}, \Gamma_{a_2}, \mathcal{A}_2) = \left( \begin{bmatrix} 1 & 0 \\ 0 & 0 \end{bmatrix}, \begin{bmatrix} 0 \\ 1 \end{bmatrix}, \mathcal{U}_2 \right)$$

for the second channel  $C_2$ , where

$$\mathcal{U}_1 := \left\{ u \in \mathbb{R}, \begin{bmatrix} u \\ 0 \end{bmatrix} \in \mathcal{U} \right\} \quad \mathcal{U}_2 := \left\{ u \in \mathbb{R}, \begin{bmatrix} 0 \\ u \end{bmatrix} \in \mathcal{U} \right\}$$

The estimated critical-time by Algorithm 1 is displayed in Fig. 4.

Table 4: Critical-time (s) - Channel-dependent scenario C1 | C2

$\gamma_1 \backslash \gamma_2$	0.55	0.575	0.60	0.625	0.65
0.65	14   9	11   12	10   10	8   8	7   6
0.675	14   7	14   10	13   12	12   10	11   8
0.70	13   6	13   9	13   12	12   11	12   9
0.725	10   5	12   8	13   11	13   12	12   10
0.75	7   4	10   7	11   10	12   14	12   11

#### 5.2.4. Interpretation

In Table 1-4, it can be observed that the choice of  $(\gamma_1, \gamma_2)$  has an important impact on the critical-time, varying from 4s to 12s in Table 3 for instance. The interest of the critical-time metric is then considered to be at least two-fold. First, it provides a means to evaluate the maximum time allocated to defense mechanisms to detect and mitigate anomalies. Second, it may be used as a prevention tool, as its maximization leads to extra-time allowed to defense mechanisms. Indeed, maximizing the critical-time may be viewed as a rational security allocation approach [4], where the aim is to tune degrees of freedom in the controlled system in order to make the security problem easier rather than developing complex defense strategies.

Finally, the estimated critical-time associated with channel-dependent sharp anomalies is especially useful for the design of the channel-isolation step, required for the selection of a suitable mitigation strategy, in a detection-and-isolation scheme [15]. Moreover, from a risk analysis perspective, it allows to identify which channel should be protected as a priority for defender with limited resources [6]. For instance, channel C2 appears here more vulnerable than C1 as it generally leads to lower critical-time (Table 4).

## 6. Conclusion

In this paper, the critical-time metric was investigated for controlled systems subject to sharp input anomalies. This metric has several advantages for off-line risk analysis as it allows for quantifying the time-window available to defense mechanisms during which safe operation can be ensured. Using the QC framework, an iterative LMI-based algorithm has been established to compute the critical-time for an uncertain linear discrete-time model. Sev-

eral classes of sharp input anomalies can be considered, depending on the input channel and the set of values the abnormal signal can take. In addition, the potential of the critical-time for risk analysis and treatment has been illustrated on the quadruple tank benchmark through the analysis of a representative set of distinct sharp anomalies scenarios.

Future work includes extension to LPV models, the investigation of the critical-time for stealthy attacks, and the integration of specific communication models.

## References

- [1] E. A. Lee, The Past, Present and Future of Cyber-Physical Systems: A Focus on Models, *Sensors* 15 (3) (2015) 4837–4869.
- [2] S. M. Dibaji, M. Pirani, D. Flamholz, A. M. Annaswamy, K. H. Johansson, A. Chakraborty, A Systems and Control Perspective of CPS Security, *Annual Reviews in Control* 47 (2019). doi:<https://doi.org/10.1016/j.arcontrol.2019.04.011>.
- [3] H. Sandberg, S. Amin, K. H. Johansson, Cyberphysical Security in Networked Control Systems: An Introduction to the Issue, *IEEE Control Systems Magazine* 35 (1) (2015) 20–23. doi:[10.1109/MCS.2014.2364708](https://doi.org/10.1109/MCS.2014.2364708).
- [4] M. S. Chong, H. Sandberg, A. Teixeira, A Tutorial Introduction to Security and Privacy for Cyber-Physical Systems, in: 2019 18th European Control Conference (ECC), 2019, pp. 968–978. doi:[10.23919/ECC.2019.8795652](https://doi.org/10.23919/ECC.2019.8795652).
- [5] D. Wang, Z. Wang, B. Shen, F. E. Alsaadi, T. Hayat, Recent Advances on Filtering and Control for Cyber-Physical Systems under Security and Resource Constraints, *Journal of the Franklin Institute* 353 (11) (2016) 2451–2466.
- [6] A. Teixeira, K. C. Sou, H. Sandberg, K. H. Johansson, Secure Control Systems: A Quantitative Risk Management Approach, *IEEE Control Systems Magazine* 35 (1) (2015) 24–45. doi:[10.1109/MCS.2014.2364709](https://doi.org/10.1109/MCS.2014.2364709).

- [7] A. Teixeira, H. Sandberg, K. H. Johansson, Strategic Stealthy Attacks: The output-to-output  $l_2$ -gain, in: 2015 54th IEEE Conference on Decision and Control (CDC), 2015, pp. 2582–2587. doi:10.1109/CDC.2015.7402605.
- [8] A. M. H. Teixeira, Security Metrics for Control Systems, in: Safety, Security and Privacy for Cyber-Physical Systems, Springer, 2021, pp. 99–121.
- [9] Q. Zhu, T. Basar, Game-Theoretic Methods for Robustness, Security, and Resilience of Cyberphysical Control Systems, IEEE Control Systems Magazine 35 (1) (2015) 46–65. doi:10.1109/MCS.2014.2364710.
- [10] C. Escudero, P. Massioni, G. Scorletti, E. Zamaï, Security of Control Systems: Prevention of Aging Attacks by means of Convex Robust Simulation Forecasts, IFAC-PapersOnLine 53 (2020).
- [11] C. Murguia, I. Shames, J. Ruths, D. Nešić, Security Metrics and Synthesis of Secure Control Systems, Automatica 115 (2020).
- [12] H. Fawzi, P. Tabuada, S. Diggavi, Secure Estimation and Control for Cyber-Physical Systems Under Adversarial Attacks, IEEE Transactions on Automatic Control 59 (6) (2014) 1454–1467. doi:10.1109/TAC.2014.2303233.
- [13] J. Börner, F. Steinke, Measuring LTI System Resilience against Adversarial Disturbances based on Efficient Generalized Eigenvalue Computations, in: 2021 IEEE Conference on Decision and Control (CDC), 2021.
- [14] A. Perodou, C. Combastel, A. Zolghadri, Critical-Time Analysis of Cyber-Physical Systems subject to Actuator Attacks and Faults, in: 2021 IEEE Conference on Decision and Control (CDC), 2021.
- [15] I. Hwang, S. Kim, Y. Kim, C. E. Seah, A Survey of Fault Detection, Isolation, and Reconfiguration Methods, IEEE Transactions on Control Systems Technology 18 (3) (2010) 636–653. doi:10.1109/TCST.2009.2026285.

- [16] P. Griffioen, S. Weerakkody, B. Sinopoli, O. Ozel, Y. Mo, A Tutorial on Detecting Security Attacks on Cyber-Physical Systems, in: 18th European Control Conference (ECC), IEEE, 2019.
- [17] Y. Zhang, J. Jiang, Bibliographical Review on Reconfigurable Fault-Tolerant Control Systems, *Annual Reviews in Control* 32 (2) (2008) 229–252.
- [18] A. Perodou, C. Combastel, A. Zolghadri, Towards Anomaly-Tolerant Systems by Dissipation Block Synthesis, in: 2021 5th International Conference on Control and Fault-Tolerant Systems (SysTol), IEEE, 2021, pp. 19–24.
- [19] R. Romagnoli, P. Griffioen, B. H. Krogh, B. Sinopoli, Software Rejuvenation under Persistent Attacks in Constrained Environments, *IFAC-PapersOnLine* 53 (2) (2020) 4088–4094.
- [20] D. Ye, S. Luo, A Co-Design Methodology for Cyber-Physical Systems under Actuator Fault and Cyber Attack, *Journal of the Franklin Institute* 356 (4) (2019) 1856–1879.
- [21] S. P. Boyd, L. El Ghaoui, E. Feron, V. Balakrishnan, *Linear Matrix Inequalities in System and Control Theory*, Vol. 15, SIAM, 1994.
- [22] K. H. Johansson, The Quadruple-Tank Process: a Multivariable Laboratory Process with an Adjustable Zero, *IEEE Transactions on Control Systems Technology* 8 (3) (2000) 456–465. doi:10.1109/87.845876.
- [23] M. Althoff, G. Frehse, A. Girard, Set Propagation Techniques for Reachability Analysis, *Annual Review of Control, Robotics, and Autonomous Systems* 4 (2021) 369–395.
- [24] U. T. Jönsson, A lecture on the S-procedure, *Lecture Note at the Royal Institute of technology, Sweden* 23 (2001) 34–36.
- [25] G. Scorletti, *Approche Unifiée de l’Analyse et de la Commande des Systemes par Formulation LMI*, Ph.D. thesis (1997).  
URL [www.theses.fr/1997PA112160/document](http://www.theses.fr/1997PA112160/document)
- [26] H. S. Sánchez, D. Rotondo, T. Escobet, V. Puig, J. Quevedo, Bibliographical Review on Cyber Attacks from a Control Oriented Perspective, *Annual Reviews in Control* 48 (2019) 103–128.

- [27] H. S. Sanchez, D. Rotondo, T. Escobet, V. Puig, J. Saludes, J. Quevedo, Detection of Replay Attacks in Cyber-Physical Systems using a Frequency-based Signature, *Journal of the Franklin Institute* 356 (5) (2019) 2798–2824.
- [28] M. Grant, S. Boyd, CVX: Matlab Software for Disciplined Convex Programming, version 2.2, <http://cvxr.com/cvx> (Mar. 2020).
- [29] MOSEK ApS, The MOSEK optimization toolbox for MATLAB manual. Version 9.3 (2021).
- [30] L. Schenato, B. Sinopoli, M. Franceschetti, K. Poolla, S. S. Sastry, Foundations of Control and Estimation Over Lossy Networks, *Proceedings of the IEEE* 95 (1) (2007) 163–187. doi:10.1109/JPROC.2006.887306.